[October, 1979] BULLETIN OF THE CHEMICAL SOCIETY OF JAPAN, VOL. 52 (10), 2747—2751 (1979) 2747

Molecular Structure of Bromoform as Determined by a Joint Analysis of Electron Diffraction and Microwave Data†

Koichi TAMAGAWA and Masao KIMURA*
Department of Chemistry, Faculty of Science, Hokkaido University, Sapporo 060

(Received August 2, 1978)

The gas phase molecular structure of bromoform has been studied by electron diffraction. By a joint analysis of the diffraction results and the moments of inertia for $CH^{79}Br_3$, $CD^{79}Br_3$, $CH^{81}Br_3$, and $CD^{81}Br_3$ obtained by Williams *et al.*, the bond distances in r_g and the bond angles in φ_{av} have been determined as follows: r_g(C–Br) = 1.924±0.005 Å, r_g(Br···Br) = 3.175±0.003 Å, r_g(C–H) = $1.11_1 \pm 0.04_6$ Å, φ_{av}(BrCBr) = 111.7±0.4°, and φ_{av}(HCBr) = 107.2±0.5°. The uncertainties represent the estimated limits of error. The anharmonicity parameter of the Morse-type potential, a_3, for the nonbonded Br···Br atom pair has been estimated as -1.3 ± 0.9 Å^{-1}.

In a series of fluoromethanes, $CH_{4-n}F_n$ (n=1—4), the systematic decrease in the C–F distances and the F–C–F bond angles with an increase in the number of F atoms has been observed.[1–4] The results of population analysis for these compounds have supported these trends.[6] According to our recent studies on a series of chloromethanes,[7–9] the C–Cl distances have shown a similar shortening with increasing number of Cl atoms, while the Cl–C–Cl bond angles increase in contrast with the trend observed in fluoromethanes.

In the molecular structures of the bromomethanes, $CH_{4-n}Br_n$ (n=1—4), only the r_e structure of CH_3Br investigated by Duncan[1] and the r_a structure of CH_2Br_2 determined by Beagley *et al.*[5] have been reported. The molecular structure of $CHBr_3$ was studied by Morino *et al.* by means of the visual method of electron diffraction[10] and by Williams *et al.* by means of microwave spectroscopy.[11] The results of structural analysis for $CHBr_3$ are however not precise and accurate enough to be compared critically with those of related molecules. There is no reliable structural data for CBr_4. Thus, in order to investigate the variations in structure with the number of bromine atoms, it is necessary to determine the structures of $CHBr_3$ and CBr_4 and moreover, it is desirable to reinvestigate the structures of CH_2Br_2 and CH_3Br in a series of studies. In the present study the structure of $CHBr_3$ was determined by a joint analysis of the diffraction data newly obtained and the rotational constants determined by Williams *et al.*[11] The structures of carbon tetrabromide,[12] methylene dibromide,[12] and methyl bromide[13] will be reported later.

Experimental

A guaranteed reagent purchased from Nakarai Chemical Co., Ltd. was used after distillation. Diffraction photographs were taken at 19 °C with a diffraction unit equipped with an r^3-sector.[14] The experimental conditions were as follows: camera length: 244.3 and 109.3 mm; sample pressure: about 3 Torr; exposure times: about 120 and 240 s for the long and

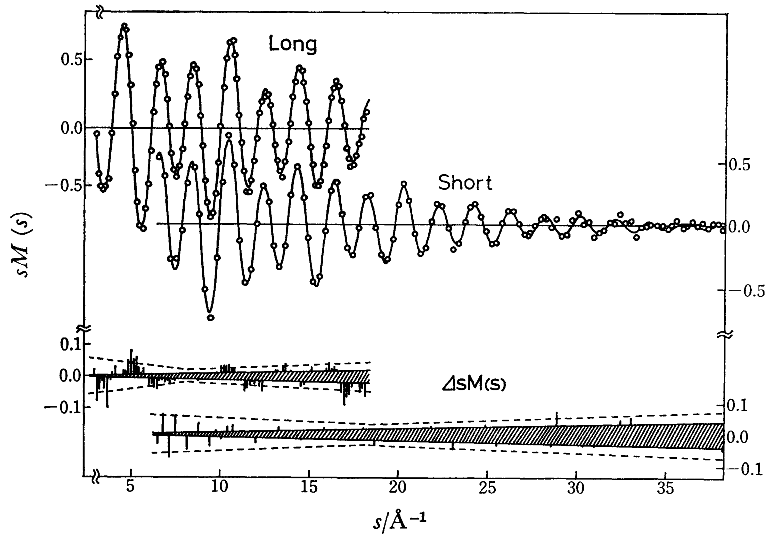

Fig. 1. Experimental (open circles) and theoretical (smooth curve) molecular intensities for $CHBr_3$; $\Delta sM(s) = sM(s)^{obsd} - sM(s)^{calcd}$. The indices of resolution are 0.918—0.967 and 0.869—0.928 for the long and short camera lengths, respectively.

---

† Throughout this paper 1 Å = 100 pm and 1 Torr = 133.322 Pa are used. For the definitions of various distances, see, *e.g.*, K. Kuchitsu and S. J. Cyvin, "Molecular Structures and Vibrations," ed by S. J. Cyvin, Elsevier, Amsterdam (1972) Chap. 12; see also L. S. Bartell, K. Kuchitsu, and H. M. Seip, *Acta Crystallogr., Sect. A*, **32**, 1013 (1976). Notations r_{av} and φ_{av} are used for the values determined by joint analysis.

short camera lengths respectively; accelerating voltage: about 42 kV; beam current: 0.20 μA. The scale factor for the diffraction patterns was determined with reference to the diffraction patterns of carbon disulfide taken under the same experimental conditions.[15)]

The data were reduced to the molecular intensities by our usual procedures.[16)] Three and four plates from the long and short camera lengths, respectively, were used for analysis. The observed molecular intensities covered the ranges of $3.0 \leqq s \leqq 18.0$ Å^{-1} and $6.5 \leqq s \leqq 38.2$ Å^{-1} for the long and short camera lengths, respectively.

The observed molecular intensities and the theoretical curves calculated using the best-fit parameters are shown in Fig. 1 together with the differences (experimental minus theoretical).[17)] The narrow shaded area corresponds to ±2 in the last digit of the digital voltmeter reading, *i.e.*, the limits of detection in photometry. The outer boundaries drawn by the broken lines show the estimated limits of error in the intensity measurements. They indicate the normally expected range of random scattering of differences between experimental and theoretical intensities. Some points exceed the boundaries for accidental reasons. The least-squares refinement with zero-weights for these points showed that the irregularities did not affect the derived parameter values. Figure 2 shows the radial distribution curve corresponding to the molecular intensities from the short camera length shown in Fig. 1.

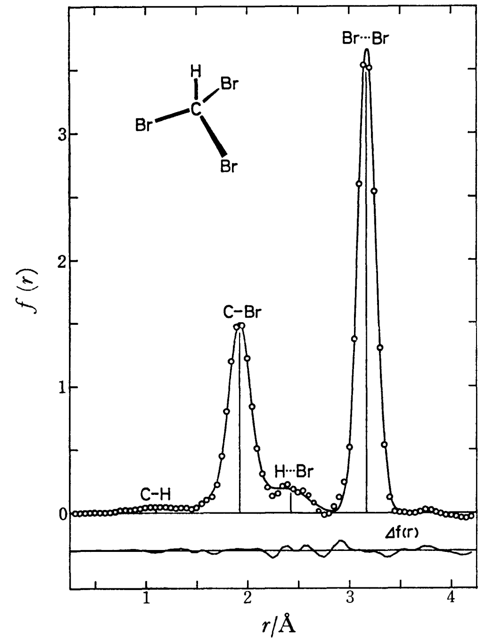

Fig. 2. Experimental (open circles) and theoretical (smooth curve) radial distribution curve for $CHBr_3$: $\Delta f(r) = f(r)^{\mathrm{obsd}} - f(r)^{\mathrm{calcd}}$. Damping factor, exp$[-0.00153\, s^2]$.

Analysis of Electron Diffraction Intensities

The structural parameters were determined by applying the least-squares method to the reduced molecular intensities with a conventional diagonal-weight matrix.[16)] The elastic and inelastic scattering factors and the phase shifts between C, H, and Br atoms were taken from the Tables of Schäfer *et al.*[18)] C_{3v} symmetry was assumed for the geometry in equilibrium. Five independent parameters were chosen for refinement: the C–Br and Br···Br distances, the mean amplitudes, and the index of resolution. The r_g(C–H) distance was fixed at 1.107 Å, a value determined from methane,[19)] and also at values shifted by ±0.050 Å. The mean amplitudes of the C–H and H···Br pairs were fixed at 0.078 and 0.113 Å, which were calculated using the force constants given by Galasso *et al.*[20)] The asymmetry constants, $\kappa (= (1/6) a_3 (1 + 8\chi/(1+\chi)^2) l^4)$, for the C–H and C–Br bonds were estimated to be 1.2×10^{-5} and 3.5×10^{-6} Å^3, assuming the anharmonicity parameters, a_3,[21)] to be 1.98 and 2.0 Å^{-1}, respectively. The a_3 values for the nonbonded H···Br and Br···Br pairs were assumed to be zero. The results of the least-squares analysis thus obtained are summarized in Table 1. The errors in the scale factor were estimated to be 0.06% and 0.10% for the long and short camera lengths, respectively. The shifts of ±0.050 Å in an assumed r_g(C–H) value brought about changes of ±0.0012 Å in the resulting r_g(C–Br), but caused no significant changes in the other structural parameters as compared with the random errors. The limits of error for the parameter values, except for r_g(C–Br), were estimated from 2.6 times the random standard deviations and the error in the scale factor. For r_g(C–Br), the error due to the uncertainty of the r_g(C–H) distance was further added. Variations in the plausible ranges of mean amplitudes for the nonbonded pairs and κ values for the C–Br, C–H, and H···Br pairs caused no significant changes in the resulting parameter values. Variation in the κ_{BrBr} value associated with variation in a_3(Br···Br) was found to cause only a little change in the r_g(Br···Br) distance, while the a_3(Br···Br) value itself took a significant role in the determination of the r_{av} structure by the joint analysis. The details of this however will be deferred

TABLE 1. RESULTS OF THE LEAST-SQUARES ANALYSIS OF DIFFRACTION INTENSITIES FOR BROMOFORM[a)] (in Å units)

Parameter	Long	Short	Weighted average	$r_g - r_\alpha^0$ [b)]	r_α^0
r_g(C–Br)	$1.922_3(5_9)$	$1.925_3(5_8)$	$1.923_8(4_2)$	0.002_8	1.921_0
r_g(Br···Br)	$3.176_7(2_6)$	$3.174_2(3_9)$	$3.175_9(2_2)$	0.001_6	3.174_3
r_g(C–H)	[1.107±0.050]	[1.107±0.050]		$[0.014_4]$	[1.093]
l(C–Br)	$0.062_0(9_1)$	$0.051_0(8_5)$	$0.056_1(6_3)$		
l(Br···Br)	$0.074_6(5_8)$	$0.071_1(2_5)$	$0.071_7(2_4)$		
R[c)]	$0.094_3(8_1)$	$0.125_9(13_8)$			

a) Parenthesized values represent the limits of error. The values in brackets were those assumed. b) Vibrational corrections were calculated from the force constants cited in Ref. 20. a_3 for the nonbonded Br···Br pair was assumed to be 0 Å^{-1}. c) $R = \{\sum_i w_i (\Delta sM(s)_i)^2 / \sum_i w_i (sM(s)_i^{\mathrm{obsd}})^2\}^{1/2}$ where $\Delta sM(s)_i = sM(s)_i^{\mathrm{obsd}} - sM(s)_i^{\mathrm{calcd}}$.

until the next section. The structural parameters determined from the data for the long and short camera lengths agree with each other within the limits of error. The most probable parameter values from the diffraction data were determined by taking the weighted average of both results. The observed mean amplitudes for the C–Br and Br···Br pairs agree with the calculated values, 0.0533 and 0.0740 Å, respectively, within the limits of error.

Joint Analysis of Diffraction and Microwave Data

The r_g distances determined by electron diffraction were converted to r_α^0 distances using the equation:[22]

$$r_g - r_\alpha^0 \cong \left(\frac{3}{2}\right) a_3(\langle \Delta z^2 \rangle_T - \langle \Delta z^2 \rangle_0) + \frac{\langle \Delta x^2 \rangle_0 + \langle \Delta y^2 \rangle_0}{2r_g} + \delta r_{\text{cent}}$$

The corrections were calculated using the force constants determined by Galasso *et al.*,[20] and the $r_g - r_\alpha^0$ values thus obtained are listed, together with the r_α^0 values in Table 1.

The ground state rotational constants, B_0, for $CH^{79}Br_3$, $CD^{79}Br_3$, $CH^{81}Br_3$, and $CD^{81}Br_3$ have been determined by Williams *et al.* using microwave spectroscopy.[11] The B_0 values were converted to the effective moments of inertia, $I_b^{(\text{eff})}$. The $I_b^{(\text{eff})}$ values thus obtained were reduced to the zero-point average moments of inertia, $I_b^{(z)}$, by correcting for harmonic vibrations by the standard method.[23]

In calculating the corrections, ΔI_b, the contribution from the centrifugal distortion was neglected[24] and the electronic contribution[24] was assumed to be zero because the *g* tensors were not available for $CHBr_3$. This assumption would not introduce significant errors, since the electronic contribution estimated from the results for formaldehyde[25] and ethylene[26] appears to be less than a few percent of the corrections themselves. A significant part of the corrections derives from terms of the $1/\omega$ type, where ω is the vibrational frequency.[27] The experimental frequencies and the frequencies calculated using the force constants agree within a few percent. Thus in the present study the overall uncertainties included in $\Delta I_b^{(z)}$ were tentatively assumed to be 10% of the correction values themselves. The uncertainties in the moments of inertia, $I_b^{(z)}$, were then estimated from the errors included in the experimental moments of inertia, $I_b^{(\text{eff})}$, and the errors included in the corrections, $\Delta I_b^{(z)}$. Table 2 lists the results.

The isotope effects for the bond distances were estimated using the equation:[28]

$$\delta r_z \cong \left(\frac{3}{2}\right) a_3 \delta \langle \Delta z^2 \rangle_0 - \delta(\langle \Delta x^2 \rangle_0 + \langle \Delta y^2 \rangle_0)/2r_z$$

Assuming the anharmonicity parameters, a_3, to be 2.0 ± 0.5 and 1.98 ± 0.5 Å^{-1} for C–Br and C–H, respectively, the isotopic differences were estimated to be -0.0009 ± 0.0015 Å for δr_z(C–D) (r_z(C–D) minus r_z(C–H)). The secondary isotope effect for r_z(C–H) and the primary and secondary isotope effects for r_z(C–Br) were estimated to be of the order of 1×10^{-6} Å, and consequently were neglected in the analysis. The isotope effect for the Br–C–Br bond angle, $\delta\varphi_z$(BrCBr) (φ_z of the isotopic species minus φ_z of the parent species $CH^{79}Br_3$), was tentatively assumed for all isotopic species to be $0.00 \pm 0.01°$ because of a lack of an established method of estimation.

TABLE 3. r_{av} AND THE FINAL r_g STRUCTURE FOR $CHBr_3$[a] (in Å and degree units)

	r_{av} and φ_{av}[b]	r_g[c]
C–Br	$1.921_0(4_2)$	1.924(5)
Br···Br	$3.179_1(1_5)$	3.175(3)
C–H	$1.09_7(4_6)$	$1.11_1(4_6)$
BrCBr	$111.6_8(3_8)$	
HCBr	$107.1_6(4_2)$	

a) Parenthesized values represent the limits of error referred to the last digits. b) Calculated from the r_{av} distances. c) Estimated from the r_{av} distances using a_3(Br···Br) $= -1.3 \pm 0.9$ Å^{-1}.

Four moments of inertia, $I_b^{(z)}$, are available. Unfortunately however the Br isotopic species provide no independent information, as we have usually experienced for molecules containing heavier atoms. The observed $I_b^{(z)}$ give relations among three parameters (r_z(C–Br), r_z(Br···Br), and r_z(C–H)). The relations from $CH^{79}Br_3$ and $CD^{79}Br_3$ practically coincide however with those from $CH^{81}Br_3$ and $CD^{81}Br_3$, respectively. Therefore, a complete r_z structure cannot be determined by the microwave data alone. The process of joint analysis to determine the complete r_{av} structure is illustrated in Fig. 3, where the r_z(C–Br)—r_z(Br···Br) space is spread out. Assigning r_z(C–H) at a certain value, an approximately linear relation between r_z(C–Br) and r_z(Br···Br) is defined by a given $I_b^{(z)}$

TABLE 2. EXPERIMENTAL MOMENTS OF INERTIA, VIBRATIONAL CORRECTIONS AND CALCULATED MOMENTS OF INERTIA FOR $CHBr_3$[a]

	$CH^{79}Br_3$	$CD^{79}Br_3$	$CH^{81}Br_3$	$CD^{81}Br_3$
B_0[b]	1247.61(3)	1239.45(3)	1217.30(3)	1209.51(8)
$I_b^{(\text{eff})}$[c]	$405.08_7(2_8)$	$407.75_4(2_8)$	$415.17_4(2_9)$	$417.84_8(2_9)$
ΔI_b	$0.08_8(0_9)$	$0.08_5(0_9)$	$0.08_8(0_9)$	$0.08_5(0_9)$
$I_b^{(z)}$[d]	$405.17_5(3_0)$	$407.83_9(3_0)$	$415.26_2(3_1)$	$417.93_3(3_1)$
$I_b^{(av)}$[e]	405.17_2	407.83_4	415.26_8	417.93_7

a) Units of B_0 are MHz and those of I are amu Å^2. Conversion factor, 505391 amu Å^2 MHz. Parenthesized values are estimated errors. b) Taken from Ref. 11. c) The errors of $I_b^{(\text{eff})}$ were taken to be 3 times the errors of B_0. d) Average moments of inertia ($I_b^{(z)} = I_b^{(\text{eff})} + \Delta I_b$). e) Calculated from the final average structures.

for each of the H- and D-species. The observed $I_b^{(z)}$ for both species and the isotope species, δr_z(C–D) and δr_z(Br···Br) for the D-species possess uncertainties however and the relationships between r_z(C–Br) and r_z(Br···Br) for both species are manifested by two approximately straight belts on the r_z(C–Br)-r_z(Br···Br) space. Thus, a parallelogram, formed by the crossing of the two belts is the range allowed by $I_b^{(z)}$ for the r_z(C–H) value. Two parallelograms, a and b, are depicted in Fig. 3 by broken lines as examples, indicating the allowed ranges for r_z(C–H) values of 1.060 and 1.140 Å, respectively. Setting different values of r_z(C–H) shifts the parallelogram along the two parallel lines M_1 and M_2. The point ED in Fig. 3 represents the r_α^0 structure determined by electron diffraction with a_3(Br···Br) equal to zero, and the elliptical curve indicates the limits of error. The ranges satisfying the electron diffraction data and the moments of inertia from microwave spectroscopy do not overlap. Among the parameter values assumed in the present analysis the most ambiguous and influential one is a_3(Br···Br). The inconsistency between the electron diffraction data and the microwave data is in all probability due to the assumption that a_3(Br···Br) is zero. Variation in the value of a_3(Br···Br) affects the isotopic differences, δr_z(Br···Br), and consequently the range between M_1 and M_2 shifts. This shifts however is small and cannot be depicted in Fig. 3 discriminately. Variation in the value of a_3(Br···Br) causes a small change in the r_g(Br···Br) distance and a relatively large change in the correction value, r_g(Br···Br) − r_α^0(Br···Br). As a result, the point ED and consequentry the elliptical curve (error limits) in Fig. 3 shifts along the Br···Br axis without influencing the other parameter values. As an example, a change in the a_3(Br···Br) value of -1.0 Å^{-1} brings about changes of -0.0011, -0.0047, and 0.0036 Å in r_g(Br···Br), the correction, r_g(Br···Br)$-r_\alpha^0$(Br···Br), and r_α^0(Br···Br) respectively. The two ellipses, ED_1 and ED_2, depicted by the dotted lines are the extreme cases where the results from both electron diffraction and microwave data overlap, corresponding to the a_3(Br···Br) values of -0.4 and -2.2 Å^{-1}, respectively. The shaded area is the range allowed by both the diffraction and the microwave data, assuming the a_3(Br···Br) value takes the range discussed above. On the basis of this, the most probable average distances, r_{av}(Br···Br) and r_{av}(C–Br), and the limits of error were determined from the center, O, and the boundary of the shaded area in Fig. 3. The most probable value for r_{av}(C–H) was taken as the value that brings the center of the parallelogram to the point O, and the limit of error was taken as the range where the parallelogram overlaps with the shaded area. The r_{av} values thus determined are listed in Table 3. The most probable value of a_3 and error limit are -1.3 ± 0.9 Å^{-1} from values corresponding to the extreme cases, ED_1 and ED_2. As may be seen in Table 3 and also in Fig. 3, r_{av}(C–H) cannot be determined precisely. Most of the r_g(C–H) distances reported so far for several molecules are in the range 1.100—1.110 Å, which corresponds to 1.085—1.095 Å in r_{av}(C–H). Even though the range of r_{av}(C–H) in the present molecule is limited to the range mentioned above, the limit of error for the r_{av}(Br···Br) becomes smaller by only 0.0003 Å. The calculated moments of inertia corresponding to the r_{av} structure are compared with the observed moments of inertia in the bottom row of Table 2. The r_g(Br···Br) distance converged

TABLE 4. C–H DISTANCES AND BOND ANGLES OF BROMOFORM AND RELATED MOLECULES$^{a)}$ (in Å and degree units)

Molecule	Method		r(C–H)	XCX$^{b)}$	Ref.
HCF_3	MW	r_0	1.098	108.80(75)	4
$HCCl_3$	ED+MW	r_g	1.136(35)	110.0(2)	8
$HCBr_3$	ED+MW	r_g	$1.11_1(4_6)$	111.7(4)	c)
HCI_3	ED	r_g	—	112.0(11)	29
HCH_3	ED	r_g	1.107(1)	109.5	19
$HC(CH_3)_3$	MW	r_s	1.108(1)	111.15(10)	30
$HC(NO_2)_3$	ED	r_a	—	110.7(10)	31

a) Numbers in parentheses represent uncertainties quoted in the original papers. b) For $HCCl_3$ and $HCBr_3$, φ_{av}. For the other molecules, except for methane, the angles are in the structures specified in the third column. c) The present study.

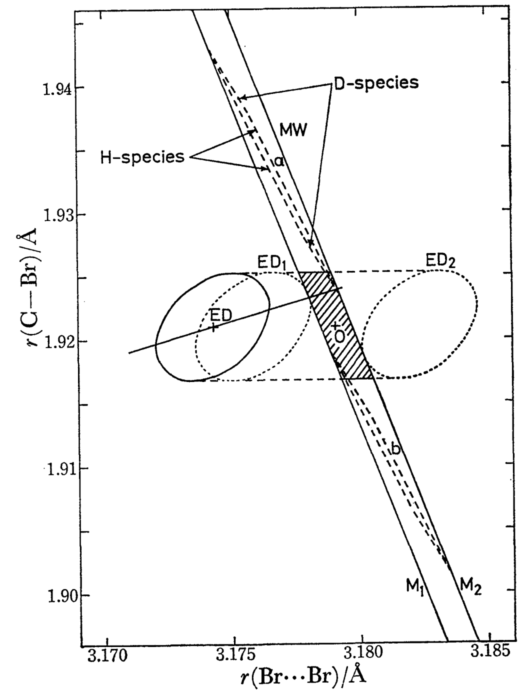

Fig. 3. The allowable range for the parameters, r(C–Br) and r(Br···Br). The values allowed by the four moments of inertia (MW) are shown by the range between the two parallel solid lines, M_1 and M_2. Two parallerograms drawn by the broken lines show the ranges allowed at r_z(C–H)=1.06 Å (a) and 1.14 Å (b), respectively. The point ED represents the r_α^0 distances determined by electron diffraction with a_3-(Br···Br) equal to 0 Å^{-1}, and the ellipse indicates the limits of error. The ellipses, ED_1 and ED_2, correspond to the a_3(Br···Br) values of -0.4 and -2.2 Å^{-1} respectively (see text). The shaded area shows the probable range of the average structure. The point O is the center of this range. The solid line passing through the point ED shows the direction of change in r(C–Br) and r(Br···Br) when the scale factor used in the electron diffraction analysis is allowed to change.

at 3.175 Å with analysis of the diffraction data assuming a_3(Br···Br) to be −1.3 Å^{-1}.

Discussion

The Br–C–Br bond angle shown in Table 3 is larger than the tetrahedral angle by about 2°. The XCX bond angles and the C–H distances of related molecules are listed in Table 4. The XCX bond angles for molecules with larger substituents are larger than the tetrahedral angle in all probability due to repulsion. A general trend for the C–H bond lengths cannot be found from the data in Table 4.

In the present study, it has been found that the anharmonicity parameter, a_3, for the nonbonded Br···Br pair must be negative in order that the electron diffraction results and the moments of inertia may be consistent. A recent study on $CHCl_3$[8] has shown that a negative a_3 values is preferable for the nonbonded Cl···Cl pair. No theoretical method for estimating these values is available at the present.

The authors wish to thank Professor Takao Iijima of Gakushuin University and Professor Shigehiro Konaka for their helpful advice and discussion. The computations were performed on an electronic computer FACOM 230-75 of the Computing Center, Hokkaido University.

References

1) J. L. Duncan, *J. Mol. Struct.*, **6**, 447 (1970).
2) E. Hirota, T. Tanaka, A. Sakakibara, Y. Ohashi, and Y. Morino, *J. Mol. Spectrosc.*, **34**, 222 (1970).
3) S. N. Ghosh, R. Trambarulo, and W. Gordy, *J. Chem. Phys.*, **20**, 605 (1952).
4) L. E. Sutton, "Tables of Interatomic Distances and Configurations in Molecules and Ions," Chemical Society, London (1958) and Supplement (1965).
5) B. Beagley, D. P. Brown, and J. M. Freeman, *J. Mol. Struct.*, **20**, 315 (1974).
6) D. P. Brown, Ph. D. Thesis, 1971, University of Manchester Institute of Science and Technology.
7) CH_2Cl_2: H. Kunimi and M. Kimura, Symposium on Molecular Structure, Tokyo, October, 1974.
8) $CHCl_3$: H. Kunimi and M. Kimura, Symposium on Molecular Structure, Nagoya, October, 1973.
9) CH_3Cl, CCl_4: K. Suzuki, Y. Todo, and M. Kimura, 35th National Meeting of the Chemical Society of Japan, Sapporo, August, 1976.
10) Y. Morino, M. Kimura, and M. Hasegawa, *Nippon Kagaku Kaishi*, **67**, 93 (1946).
11) Q. Williams, J. T. Cox, and W. Gordy, *J. Chem. Phys.*, **20**, 1524 (1952).
12) K. Tamagawa and M. Kimura, Symposium on Molecular Structure, Sapporo, August, 1977.
13) K. Tamagawa and M. Kimura, Symposium on Molecular Structure, Hiroshima, October, 1978.
14) Y. Murata, K. Kuchitsu, and M. Kimura, *Jpn. J. Appl. Phys.*, **9**, 591 (1970).
15) For the r_a(C–S) distance, see, K. Tamagawa, T. Iijima, and M. Kimura, *J. Mol. Struct.*, **30**, 243 (1976).
16) S. Konaka and M. Kimura, *Bull. Chem. Soc. Jpn.*, **43**, 1693 (1970).
17) The numerical data of the total intensity, the background, and the elements of the correlation matrix are deposited with the Chemical Society of Japan (Document No. 7928).
18) L. Schäfer, A. C. Yates, and R. A. Bonham, *J. Chem. Phys.*, **55**, 3055 (1971).
19) L. S. Bartell, K. Kuchitsu, and R. J. De Neui, *J. Chem. Phys.*, **35**, 1211 (1961).
20) V. Galasso, G. De Alti, and G. Costa, *Spectrochim. Acta*, **21**, 669 (1965).
21) K. Kuchitsu and Y. Morino, *Bull. Chem. Soc. Jpn.*, **38**, 805 (1965).
22) K. Kuchitsu and S. Konaka, *J. Chem. Phys.*, **45**, 4342 (1966).
23) K. Kuchitsu, "MTP International Review of Science, Physical Chemistry, Series One," ed by G. Allen, Medical and Technical Publishing Co. Ltd., Oxford (1972), Vol. 2, Chap. 6.
24) T. Oka and Y. Morino, *J. Mol. Spectrosc.*, **6**, 472 (1961).
25) T. Oka, *J. Phys. Soc. Jpn.*, **15**, 2274 (1960).
26) J. L. Duncan, *Mol. Phys.*, **28**, 1177 (1974).
27) T. Iijima and S. Tsuchiya, *J. Mol. Spectrosc.*, **44**, 88 (1972).
28) K. Kuchitsu, *J. Chem. Phys.*, **49**, 4456 (1968).
29) H. Sanpei and M. Kimura, preliminary result.
30) D. R. Lide, Jr., *J. Chem. Phys.*, **33**, 1519 (1960).
31) N. I. Sadova, N. I. Popik, L. V. Vilkov, Yu. A. Pankrushev, and V. A. Shlyapochnikov, *Zh. Strukt. Khim.*, **15**, 695 (1974).